RICERCA DI SISTEMA ELETTRICO

Simulazione dell'effetto di warm-prestressing su provini cruciformi

D. Bernardi

SIMULAZIONE DELL'EFFETTO DI WARM-PRESTRESSING SU PROVINI CRUCIFORMI
D. Bernardi ENEA

Settembre 2012

Titolo

SIMULAZIONE DELL'EFFETTO DI WARM PRE-STRESSING
SU PROVINI CRUCIFORMI

Descrittori

    Tipologia del documento: Rapporto Tecnico
    Collocazione contrattuale: ACCORDO DI PROGRAMMA Ministero dello Sviluppo Economico – ENEA sulla Ricerca di Sistema Elettrico PIANO ANNUALE DI REALIZZAZIONE 2011 Progetto 1.3.1: Energia nucleare: NUOVO NUCLEARE DA FISSIONE: COLLABORAZIONI INTERNAZIONALI E SVILUPPO COMPETENZE IN MATERIA NUCLEARE, PAR 2011.
    Argomenti trattati: Tecnologia dei reattori nucleari, Reattori nucleari ad acqua, Calcolo agli elementi finiti, Analisi incidentale

Sommario

Il presente rapporto descrive l'attività svolta in collaborazione col CEA di Saclay nell'ambito del progetto europeo NESC-7 sullo studio degli effetti del fenomeno di Warm Pre-Stressing (WPS) applicato al Reactor Pressure Vessel (RPV) di reattori nucleari di tipo PWR soggetti a transitori termici severi come i PTS (Pressurized Thermal Shock). Il contributo dell'ENEA ha riguardato in particolare la simulazione, mediante il codice agli Elementi Finiti CAST3M, di uno dei test sperimentali effettuati presso il CEA di Saclay su un provino cruciforme pre-intagliato sottoposto ad un ciclo di carico di tipo LCF (Load-Cool-Fracture) rappresentativo di un evento PTS. I risultati della simulazione sono stati infine confrontati con quelli ricavati sperimentalmente al fine di validare i modelli teorico-numerici utilizzati.

Summary

This report describes the activity carried out in collaboration with CEA-Saclay in the framework of the NESC-7 project for the study of the Warm Pre-Stressing (WPS) effect on a Reactor Pressure Vessel (RPV) of a PWR reactor subjected to severe thermal transients such as a Pressurized Thermal Shock (PTS). ENEA contribution concerned the simulation, through the CAST3M Finite Element code of one of the experiments performed at CEA-Saclay on a pre-cracked cruciform specimen under LCF (Load-Cool-Fracture) loading conditions reproducing a typical PTS event. Simulation results have been finally compared to experimental ones in order to validate the numerical models adopted in the analysis.

Note

Since the information concerning CEA activity are confidential, this document reports only the data that are strictly necessary to properly contextualize the ENEA contribution within NESC-7 project. For more details, refer to CEA report [8] cited in the References.

2			NOME			
			FIRMA			
1			NOME			
			FIRMA			
0	EMISSIONE		NOME	D. Bernardi	A. Aiello	M. Sepielli
			FIRMA			
REV.	DESCRIZIONE	DATA		REDAZIONE	CONVALIDA	APPROVAZIONE

Index

1. Introduction

Nuclear power plants (NPPs) equipments are subjected to a variety of ageing mechanisms. The effects of ageing can lead to a reduction in design margins and/or an increase in forced outages and repairs of components. Ageing effects in NPPs are considered in design and manufacturing specifications with some design limits in accordance with plant safety analysis. Ageing effect of the reactor pressure vessel (RPV) have the potential to be NPP life-limiting conditions for a NPP as the RPV is impossible or economically unviable to replace.

The pressurized thermal shock (PTS) issue [1], [2] is concerned with the possibility of failure of pressurized water-reactor (PWR) pressure vessels under a very specific set of conditions which include:

- Occurrence of reactor transients that subject the vessel to severe thermal shock as well as the normal pressure loading;
- Existence of sharp, crack-like defects (flaws) at the inner surface of the vessel wall;
- High enough neutron fluence and concentrations of copper and nickel in the vessel wall to result in a extensive radiation-induced reduction of the fracture toughness of the vessel material

The dominant and expected type of damage in the RPV is embrittlement under neutron irradiation, especially in the core (beltline) area. If an embrittled RPV were to have a flaw of critical size and certain severe system transients were to occur, the flaw could propagate very rapidly through the vessel, possibly resulting in a through-wall crack and challenging the integrity of the RPV.

The severe transients of concern are:

- PTS, which is characterized by a rapid cooling (i.e. thermal shock) of the down-comer and internal RPV surface, followed sometime by repressurization of the RPV. Thus, a PTS event poses a potentially significant challenge to the structural integrity of the RPV in a PWR reactor;
- Cold overpressure characterised by high pressure at a low temperature (i.e., hydro-test or end of shutdown situation).

All the potential PTS events have to be identified and safety margins against brittle fracture have to be justified in an appropriate manner. All these analyses have to be consistent with the corresponding plant safety analysis report, the design and fabrication of the RPV and the major results have to be periodically reviewed to assure consistency with maintenance activities (such as in-service inspection, surveillance programme and fluence monitoring).

RPVs are designed and manufactured to serve their purposes without rupture under normal (e.g. plant heat up and cool down), upset (e.g. reactor trip and loss of load), emergency (e.g. small loss of coolant, small steam line break or complete loss of flow) and faulted (e.g. large loss-of-coolant or large steam line break) conditions.

2. The Warm Pre-Stressing (WPS) effect

Numerous experimental results [3] on pressure vessel steels have shown that the fracture toughness can be significantly increased at low temperatures if the material is prestressed at a higher temperature. This is the so called *Warm Pre-Stressing* phenomenon. As a result, the WPS gives the material an apparent added resistance to cleavage fracture [4]. In other words, it is considered to elevate the required stress intensity factor at fracture (K_f) above the corresponding as-received fracture toughness (K_{mat}). The WPS is carried out at a temperature above the ductile-to-brittle transition temperature and at a higher temperature, or in a less brittle state, than that corresponding to the subsequent service assessment such as for example, that resulting from a PTS event. In the service assessment, the fracture toughness is therefore taken as K_f instead as K_{mat}.

Thermal shock tests of flawed components (such as those conducted under the HSST program [5]) have strongly suggested that, because of the warm prestressing phenomenon, brittle failure of nuclear reactor vessel will not occur under severe thermal shock conditions.

It is thus clear that the WPS can have important licensing implications in connection with the design lifetime of a new NPP or with the lifetime extension of an existing power reactor.

The benefits of a WPS in thick-section components have been attributed mainly to the establishment of a compressive residual stress zone ahead of the crack tip on unloading. The effects of crack-tip blunting and strain hardening have, however, also been claimed as significant by a number of authors.

In laboratory, there are usually three basic types of WPS cycle which are used to demonstrate the WPS effect (see Fig. 2-1):

(a) Load-Unload-Cool-Fracture (LUCF), where the structure is pre-loaded at temperature T_1 to stress intensity factor K_1, unloaded to stress intensity factor K_2, cooled to temperature T_2 and re-loaded to fracture.

(b) Load-Cool-Unload-Fracture (LCUF), where cooling to T_2 takes place prior to unloading and re-loading to fracture.

(c) Load-Cool-Fracture (LCF). This is similar to the LCUF cycle except that no unloading occurs prior to the imposition of extra load to fracture.
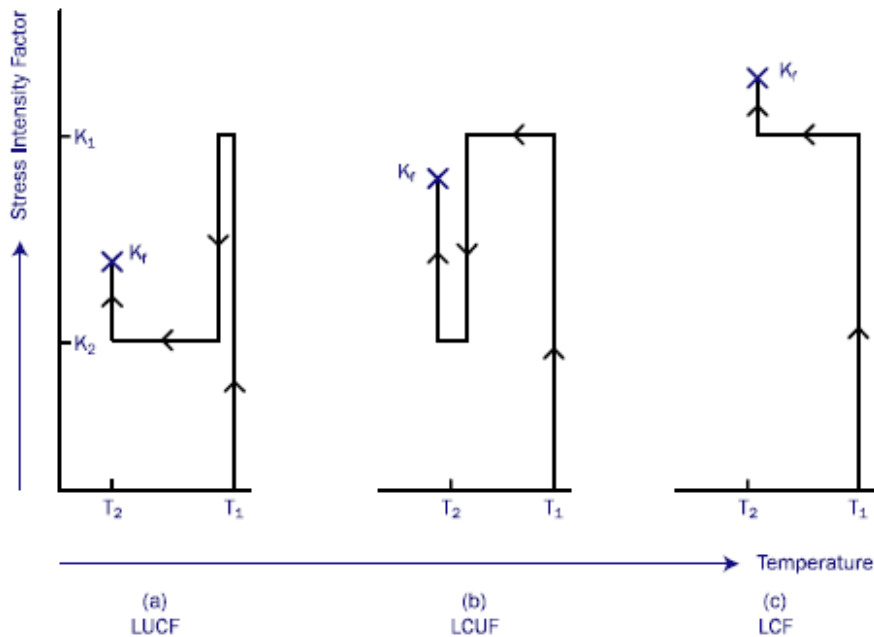

Fig. 2-1 – Typical WPS cycles

A LCF cycle was selected for the first WPS test performed by CEA within the NESC-7 programme, for which a simulation support was given by ENEA. The latter represents the object of this report.

3. ENEA-CEA collaboration within NESC-7 project

An agreement of collaboration was established between ENEA and CEA in the framework of the European NESC-7 project. This project is aimed at studying the WPS effect on specimens subjected to biaxial loading conditions representative of those arising during PTS events on reactor pressure vessels.

To reproduce such conditions, cruciform specimens [6], [7] made of 18MND5 ferritic steel (typically employed in French PWR reactor vessels) are used. The dimensions of the specimens [8] are taken in real scale with respect to those of a PWR RPV so as to perform

large scale experiments simulating realistic PTS conditions. A series of 5 bending tests were planned at CEA-Saclay LISN laboratory considering different loading paths.

In this framework, ENEA contribution is devoted to perform the post-test simulation of the first of the above series of experiments, for which a LCF loading path was employed. This path foresees a pre-loading at constant temperature T_{WPS} = -30 °C, followed by a cooling at constant load (F_{WPS} = 1328.8 kN) up to the final temperature T_{FRAC} = -150 °C and then by an isothermal reload at T_{FRAC} up to the fracture of the specimen. The values of T_{WPS}, T_{FRAC} and F_{WPS} were agreed during the 4th Progress Meeting held at Friburg in 2010, as the most appropriate parameters able to evidence the WPS effect within the LCF cycle.

The numerical tool used for the simulations is the Finite Element code CAST3M originally developed by CEA.

4. Experimental testing

4.1 Cruciform specimen

A dedicated cruciform specimen was manufactured by CEA [8] starting from a 4000 x 2000 mm, 200 mm thick, rolled plate of 18MND5 ferritic steel provided by EDF. The steel was produced by a French company (Creusot Loire Industrie) in 1995 according to RCC-M specifications. Before manufacturing, the plate was submitted to three different heat treatments (quench + tempered + stress relief heat treatment).

A semi-elliptical crack was created at the middle of the specimen (Fig. 4-1) starting from a pre-machined notch that was successively allowed to grow through fatigue pre-cracking procedure up to the desired depth. At the end of the pre-cracking phase and prior to the testing, the actual dimension of the crack was assessed using an endoscope (Fig. 4-2). This value underestimates the real crack length at the deepest point due to the "canoe effect" which is well illustrated in Fig. 4-3.
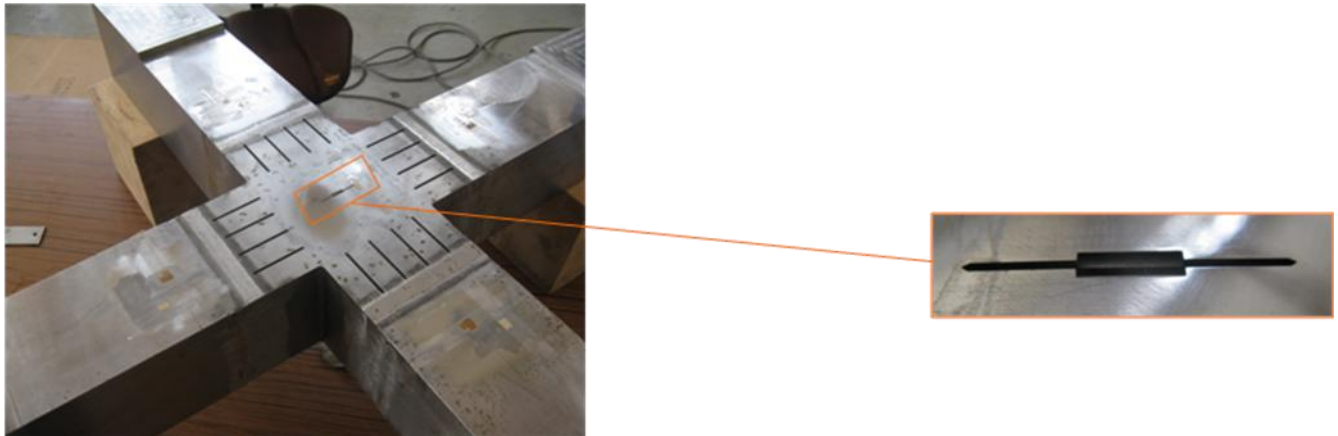
Fig. 4-1 – Cruciform specimen and detail of the crack on its surface

Therefore, after the test, the specimen was scanned and the real geometry of the crack tip was plotted.

The following crack tip dimensions were found (see Fig. 4-3):

- length **2c = 35 mm**
- depth **a = 12 mm**, corresponding to a fatigue pre cracking crack growth of 2 mm at the deepest point

The approximated crack tip elliptic geometry used in the simulation is represented by the light blue line of Fig. 4-3, which was calculated by the ellipse equation with a and c parameters given above (a = 12 mm, 2c = 35 mm).
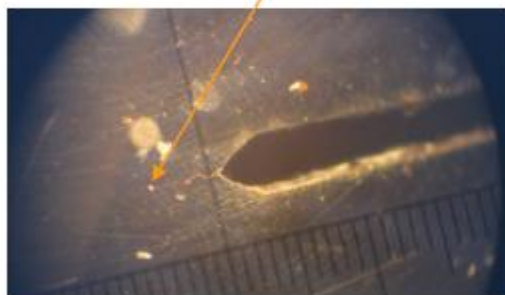

Fig. 4-2 – Crack size at the end of the fatigue pre-cracking assessed by the endoscope
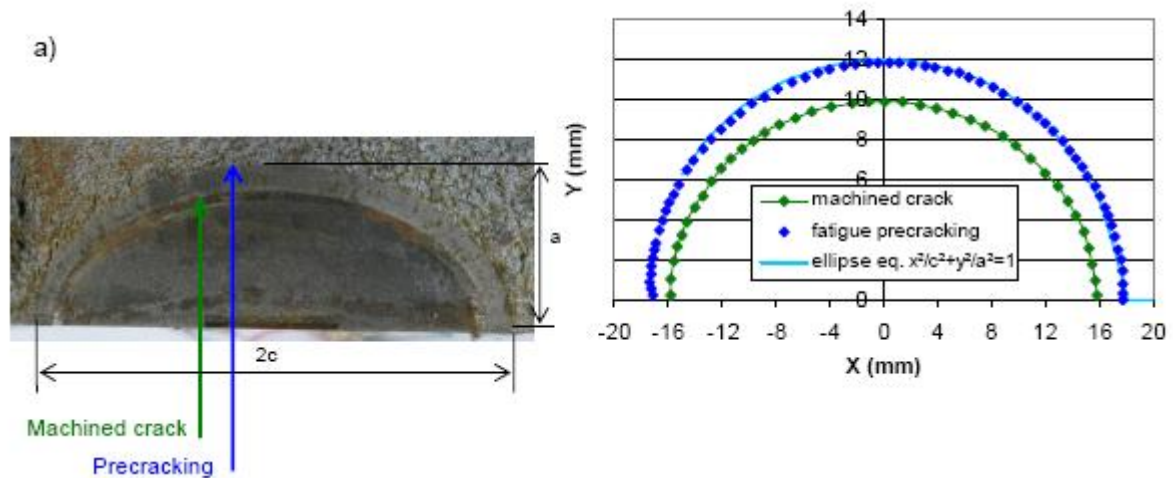
Fig. 4-3 – Post test reconstruction of crack tip geometry

4.2 *Testing equipment*

The test was performed using the following equipment available at CEA-Saclay LISN laboratory:

- a 2500 kN tensile testing machine (INSTRON) with MTS software (Fig. 4-4)

- a large thermal chamber of dimensions: 800 x 800 x 800 mm with operating temperatures: 0 to -175°C, cooled with liquid nitrogen (Fig. 4-5)

- a 5 point bending device placed into the thermal chamber, designed by the CEA and manufactured by SOMEC (Fig. 4-6). The distance between the specimen centre and a support column is L = 325 mm.

Fig. 4-4 – INSTRON 2500 kN tensile testing machine

Fig. 4-5 - Thermal chamber

Fig. 4-6 – The 5 point bending device installed inside the thermal chamber

4.3 Instrumentation and measurements

In addition to the displacements and load measured by the testing machine transducers, the following measurements were performed through the instrumentation indicated hereafter:

- Crack mouth opening displacement (CMOD) using a MTS clip gage (measuring range: 0/+4 mm, L_0 = 2.5 mm, operating temperature: -270°C/+65°C). The CMOD value given by the clip gage during the test does not correspond to the real crack opening value because of the clip gage retraction due to temperature variations. This is why it was necessary to determinate a correction equation to apply to the CMOD value measured experimentally. This equation, governing the clip gage retraction, was obtained from extra calibration tests [8].

- Specimen deflexion using a ceramic stick connected to a LVDT displacement cell (see Fig. 4-7). The deflexion measurement point is approximately located at y=5; z=0 mm as shown in Fig. 4-8. The deflexion device requires the same temperature correction as for the clip gage, to be applied to the value measured experimentally.

- Specimen temperature by taking the mean value of 3 K-type thermocouples placed close to the crack tip (Fig. 4-9-a).

- Clip gage temperature using a K-type thermocouple placed on the clip gage.

- <u>Deflexion device temperature</u> using a K-type thermocouple placed on the deflexion device.
- <u>Crack growth</u> using a crack propagation gage placed at one extremity of the crack, on the surface of the specimen (Fig. 4-8).
- <u>Check of the testing device balance</u>: using four strain gages named JC1 to JC4 placed on the 4 columns of the testing device supporting the specimen, eight low temperature strain gage located on the upper face (J1 to J4) and on the lower face (J5 to J8) of the specimen arm (Fig. 4-9-b). Two other strain gages named J2b and J6b, are placed next to respectively J2 and J6 strain gages.
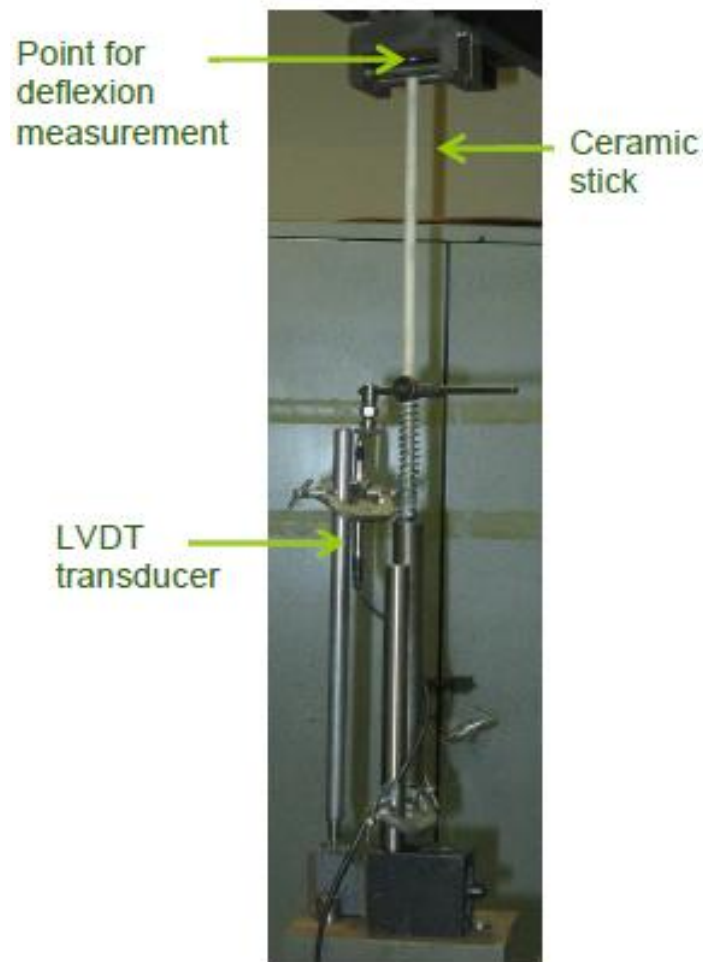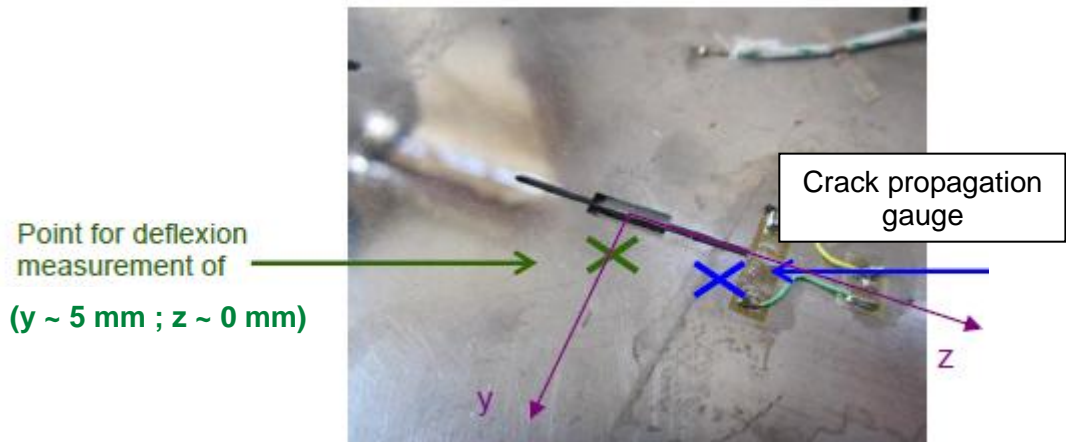

Fig. 4-7 – Specimen deflection measurement device

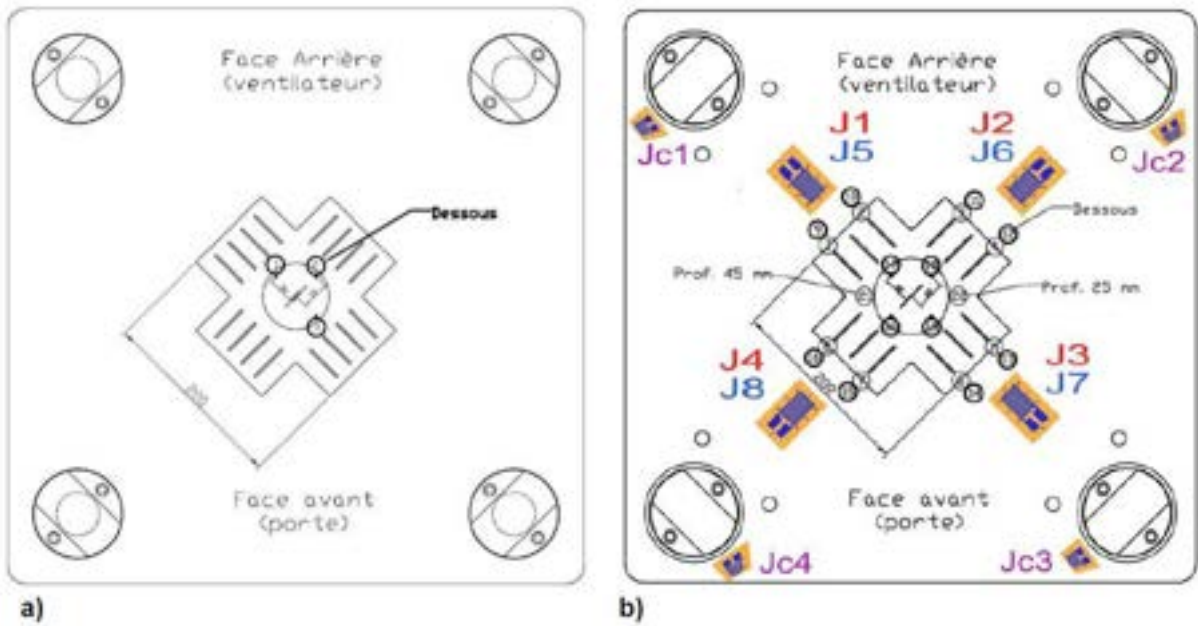Fig. 4-8 – Specimen deflection and crack growth measurement devices

Fig. 4-9 – Position of thermocouples (a) and strain gages (b)

4.4 Testing procedure

The LCF (Load-Cooling-Fracture) loading path shown in Fig. 4-10 was applied to simulate the WPS effect. The nominal testing procedure was as follows:

- Progressive cooling of the specimen down to TWPS = -30°C at approximately zero load;

- Application of WPS cycle with LCF loading path consisting of the three following steps:

  1. Pre loading up to FWPS = 1328.8 kN (corresponding to KJWPS = 80MPa m$^{1/2}$ mean value along the crack tip) with loading rate of 2 kN/s and at nominal constant temperature TWPS = -30°C

  2. Cooling down to T = -150°C at constant load F = 1328.8 kN

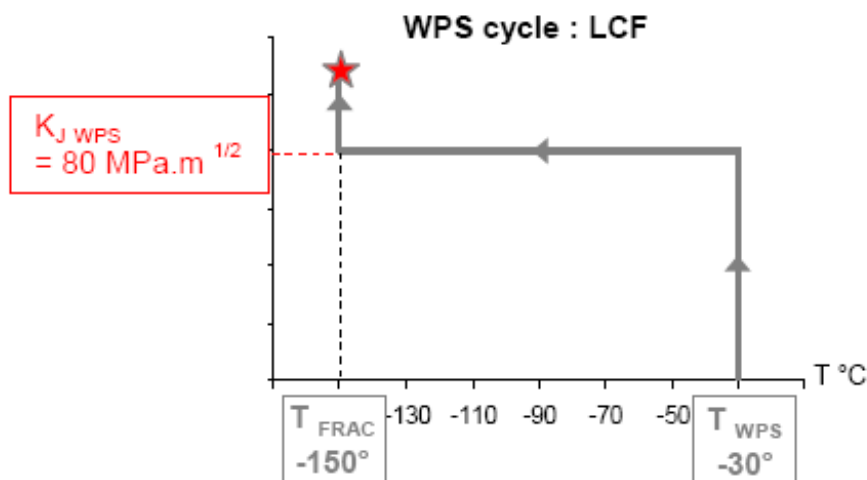 3. Reloading up to fracture at 0.1 kN/s at constant temperature T = -150°C

Fig. 4-10 - Nominal LCF loading path

4.5 Experimental results

The test was successfully carried out at CEA-Saclay laboratory in the summer 2010 in presence of an ENEA representative. Fig. 4-11 shows the bending device and the cruciform specimen after the test.

Fig. 4-11 – Specimen and bending device after the test

The results showed, as expected, the apparent increase of the fracture toughness due to the WPS effect. In fact, the fracture load was found to be:

- F_{FRACT} = 1496 kN

which corresponds to a KJ_{FRAC} well beyond the KJ_{WPS} associated to the pre-loading (F_{WPS}), being the latter higher than the value of fracture toughness corresponding to the 95% master curve at -150 °C (see Fig. 4-12). This ultimately means that $F_{FRAC} > F_{WPS}$ that clearly proves the beneficial of WPS effect.

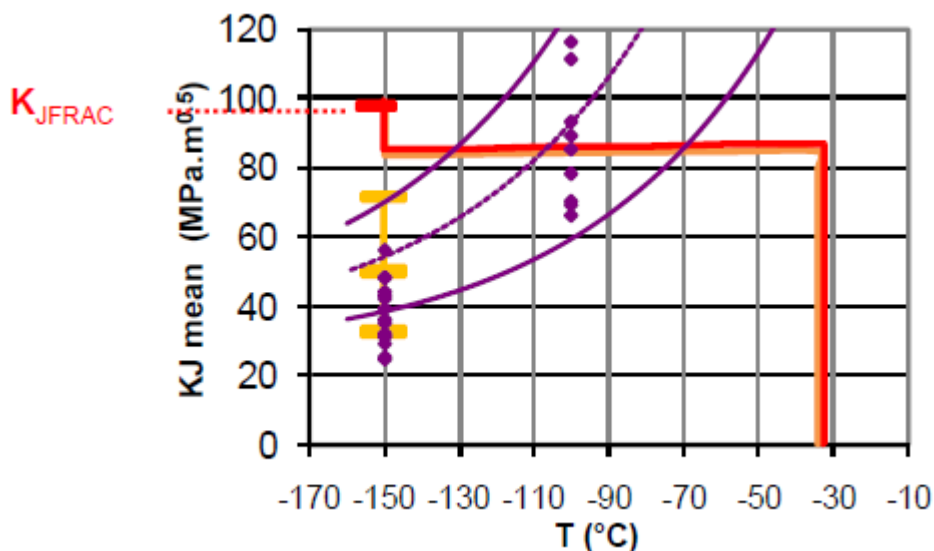

Fig. 4-12 – Demonstration of the WPS effect for a LCF cycle

At the end of the test, the specimen was visually and photografically inspected and the fracture surface was carefully examined (Fig. 4-13).

Fig. 4-13 – Fractured specimen at the end of the test

The loading path actually applied during the test is shown in Fig. 4-14 in which the load measured by the testing machine transducer (load cell) is plotted against the temperature of the specimen obtained from the dedicated thermocouples. The temperature during the isothermal pre-loading phase was found to be about -33 °C while that during reloading phase was approximately -150 °C.

The experimental results concerning the crack mouth opening displacement (CMOD) and the specimen deflection are reported in Fig. 4-15 and 4-16, respectively, as a function of the applied load.
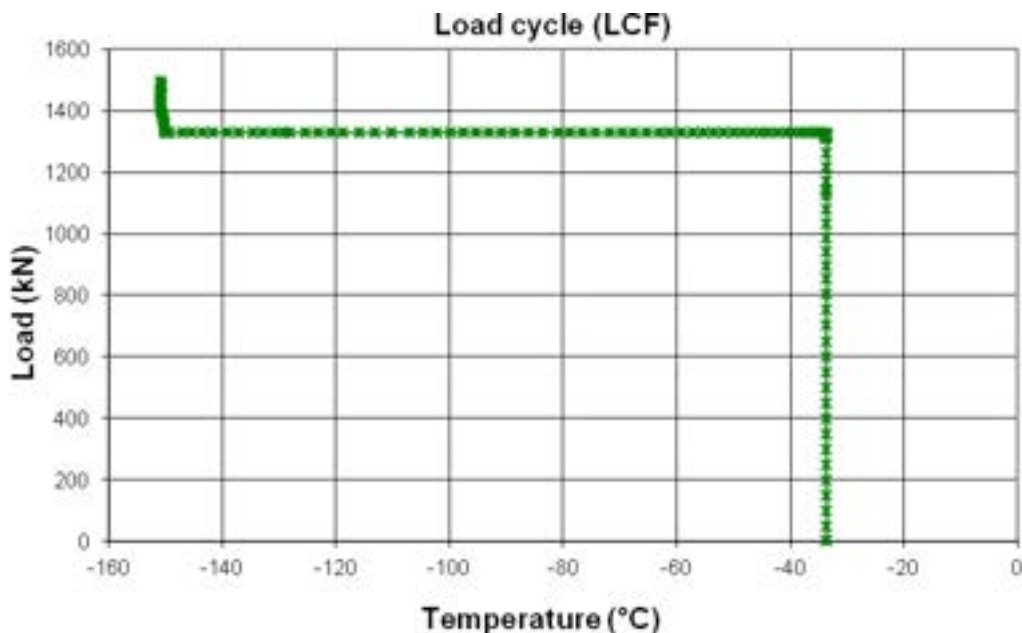

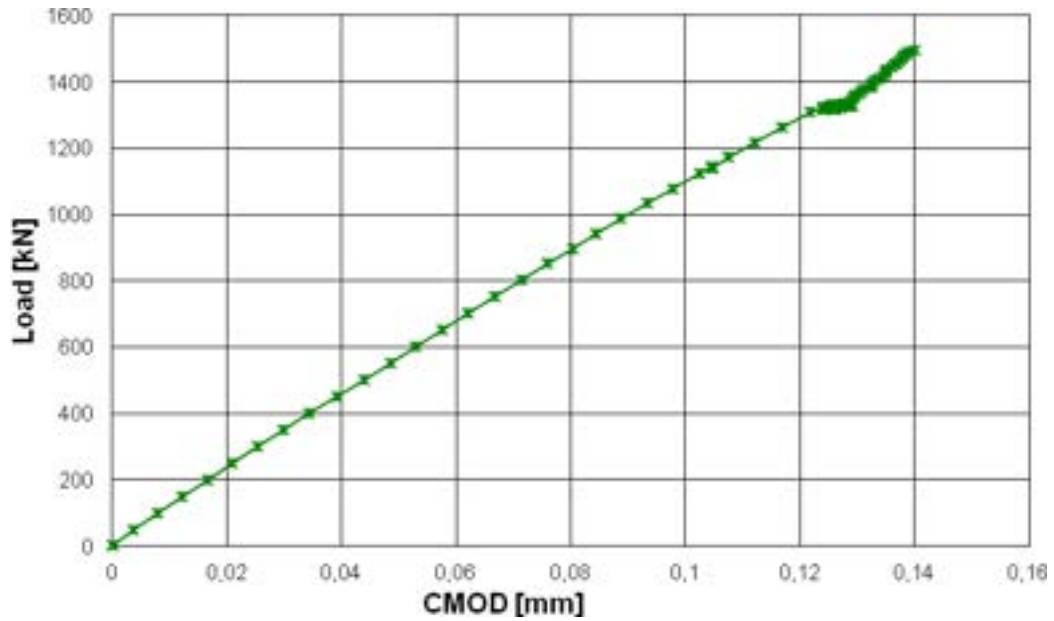Fig. 4-14 – Experimental LCF loading path

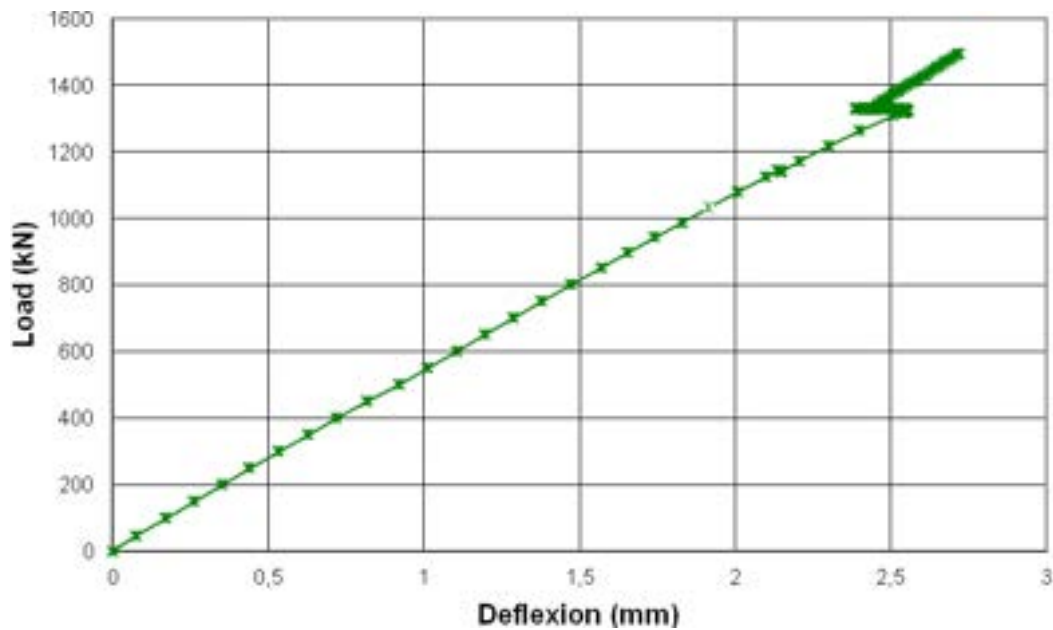Fig. 4-15 – Applied load vs. CMOD (experimental)

Fig. 4-16 – Applied load vs. specimen deflexion (experimental)

5. Numerical simulation

5.1 Geometric model and computational mesh

The geometric model was developed considering only ¼ of the specimen due to its double symmetry. The model was discretized using a regular mesh made of 3D solid cubic elements with 20 nodes (Fig. 5-1).
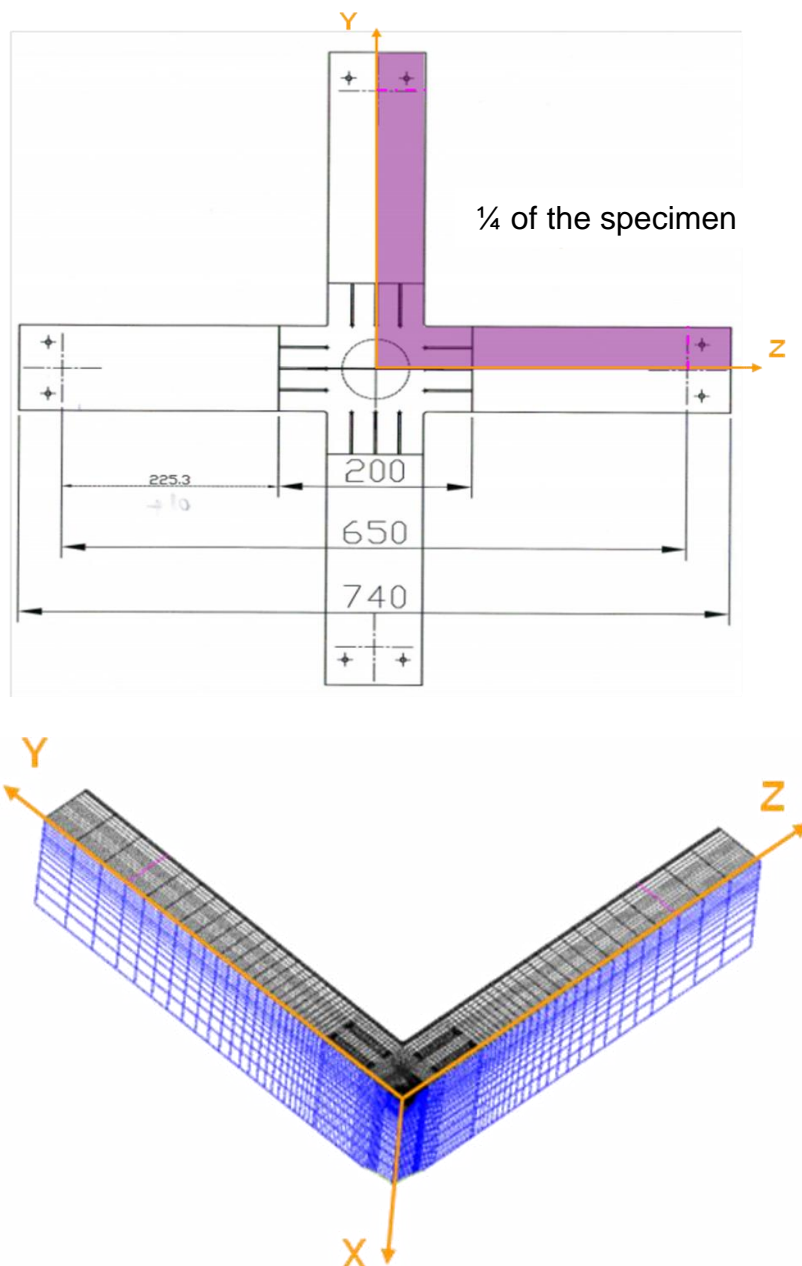

Fig. 5-1 – 3D model of the specimen

To generate the mesh, the entire volume of the model was divided into three main subvolumes (Fig. 5-2):

- The crack-box (in violet)
- The cruciform part (in dark and light blue)
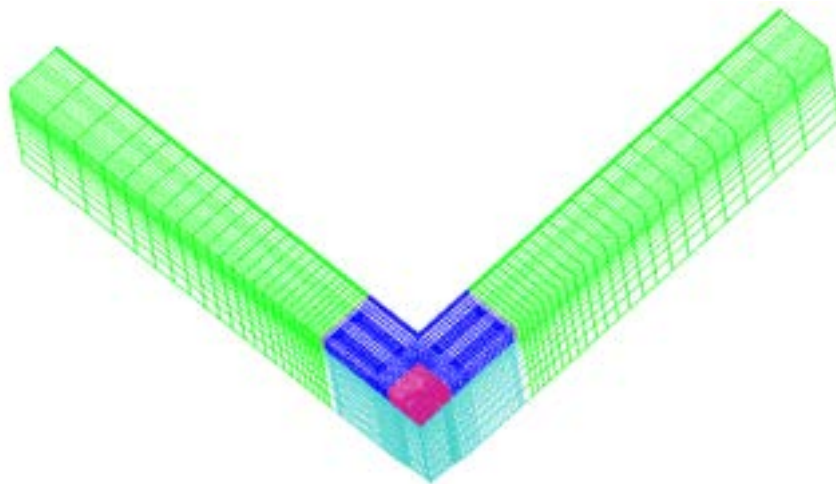- The arms (in green)

Fig. 5-2 – 3D model with its subvolumes

The crack box, shown in Fig. 5-3, is the subvolume that encompasses the elliptical crack. A very fine mesh was generated at the crack-tip (Fig. 5-4) in order to be able to describe the solution fields (displacements, stress and deformations) in this region with sufficient accuracy.
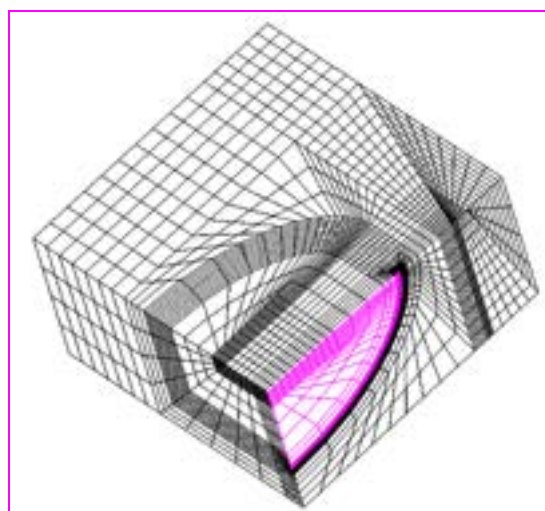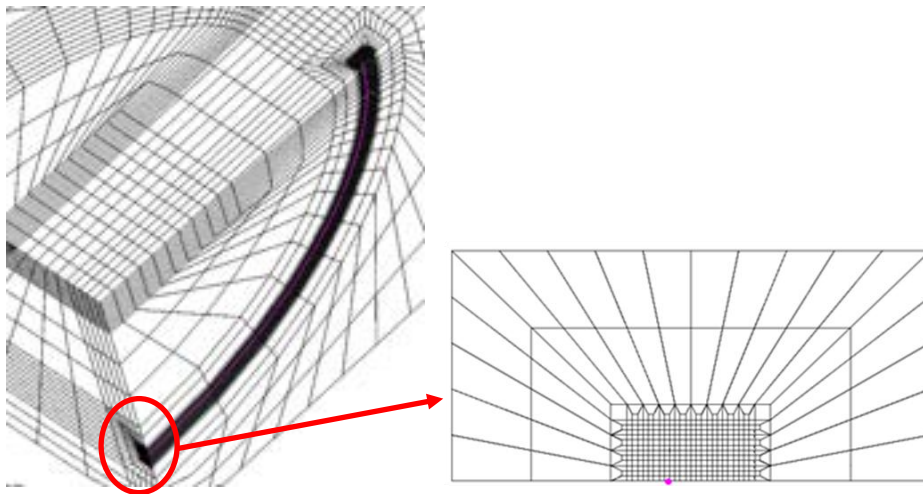

Fig. 5-3 – Crack-box

Fig. 5-4 – Refinement of the mesh at the crack-tip

The cruciform subvolume was created by first generating the two upper parts attached to the crack-box (in dark blue in Fig. 5-5) and then creating, by translation, the bottom part (in light blu in Fig. 5-5). Finally, on this latter part, a portion of spherical shape was then removed from the lower surface in order to create the zone where the load is applied (in the real experiment) or constraints are imposed (in the simulation).
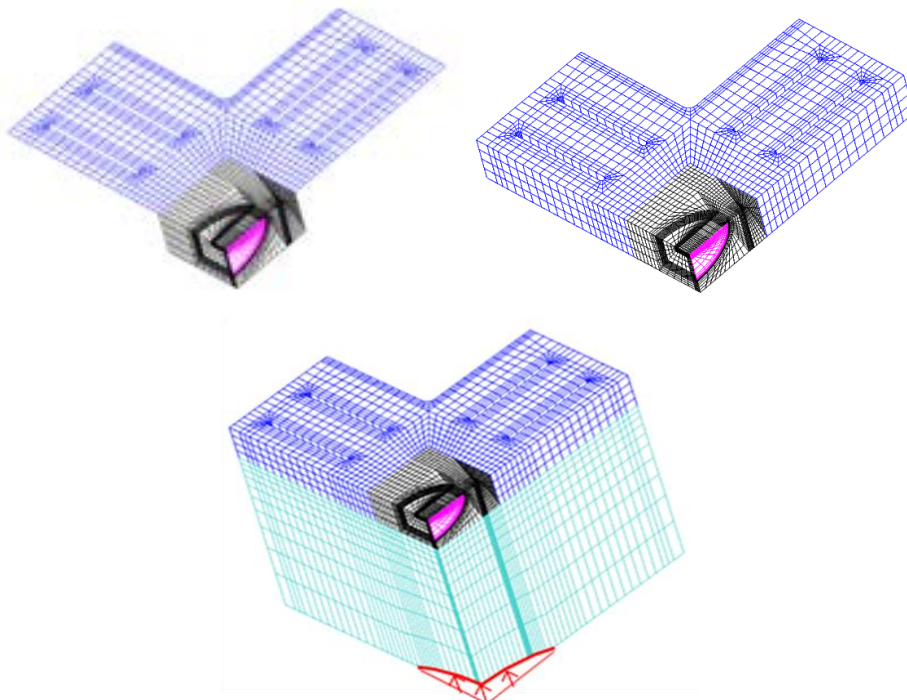

Fig. 5-5 – Generation of the cruciform subvolume and of the spherical region

In the last stage, the two arms of the model were created. The first arm was obtained by simply translating the lateral external surface of the cruciform part (see green zone in Fig. 5-6), while the second one is created by duplicating the first in a specular way with respect to the plane of symmetry of the specimen (Fig. 5-7).
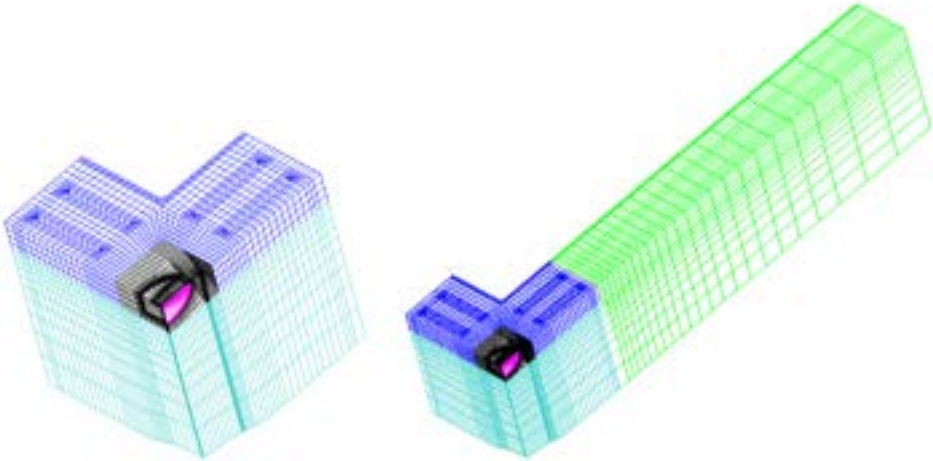

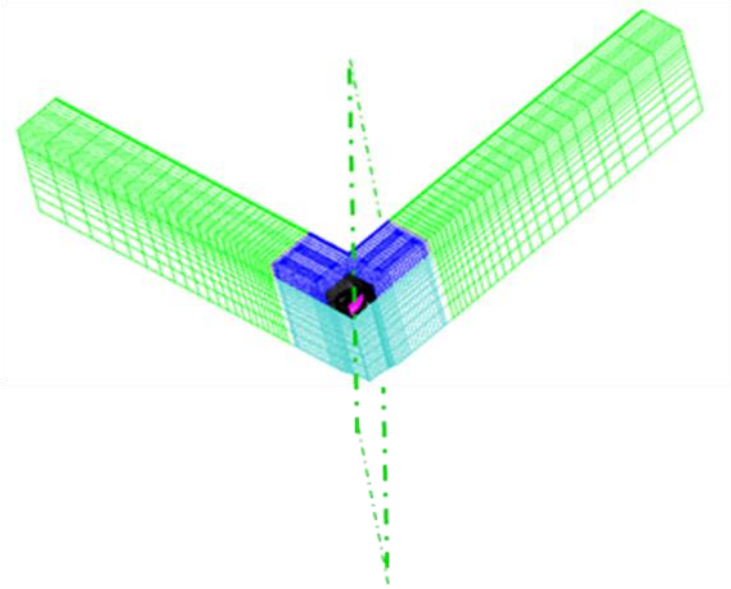Fig. 5-6 – Generation of the first specimen arm

Fig. 5-7 – Generation of the second specimen arm

5.2 Boundary conditions

To facilitate the modelling, the position of the loads and constraints in the simulation were reversed with respect to the real situation, i.e., the loads were applied on the specimen arms at the level of the contact lines with the supports while the constraints were imposed on the spherical region on which the load is actually applied in the real experiment (Fig. 5-8).

A uniformly distributed linear load was applied on each loading line while the following set of constraints were applied:

- Null displacements in x direction ($u_x = 0$) on the spherical region
- Null displacements in y direction ($u_y = 0$) on XZ plane surface (symmetry condition)
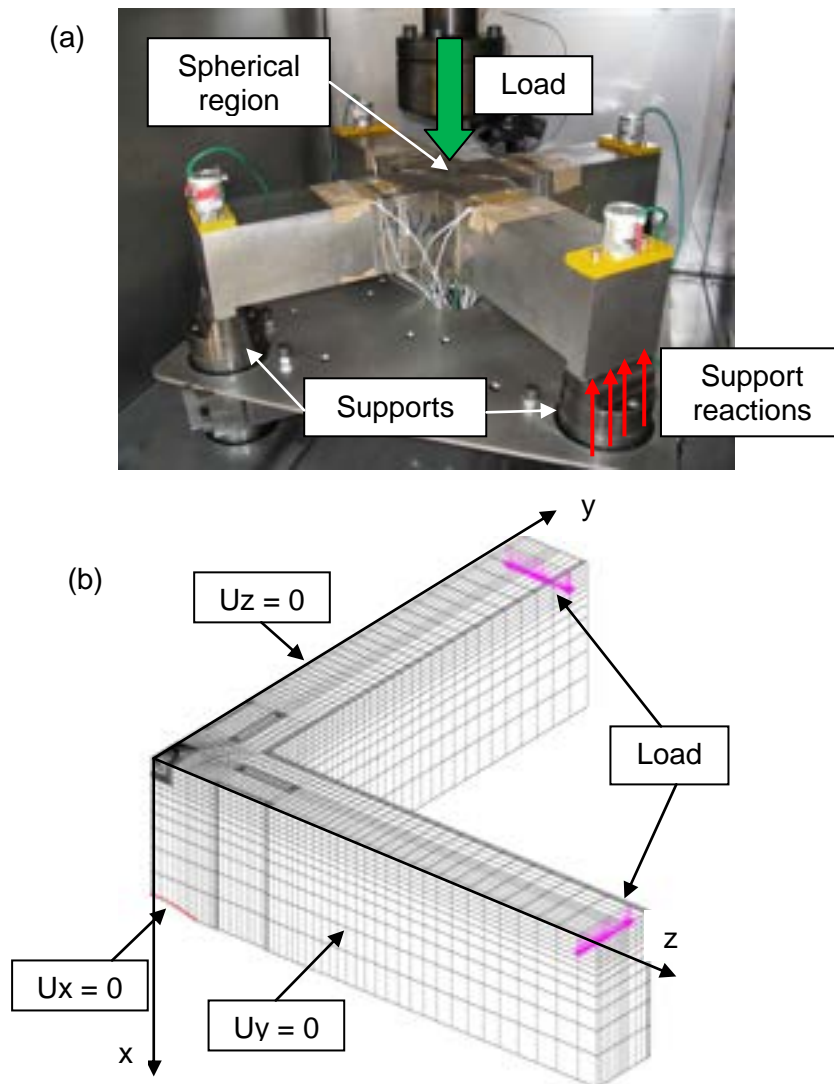- Null displacements in z direction ($u_z = 0$) on XY plane surface (symmetry condition)

Fig. 5-8 - Load and constraints configuration in the real case (a) and in the simulation (b)

5.3 Material properties

All the material properties of the 18MND5 ferritic steel needed for the analysis (tensile stress-strain curves, Young modulus, thermal expansion coefficient, poisson ratio) were supplied by CEA to all participants to the NESC-7 project.

The tensile properties were given as a set of stress-strain curves at different temperatures (-196 °C, -150 °C, -120 °C, -100 °C, -50 °C, -20 °C, 20 °C) obtained from tensile tests carried out on specimens extracted from the same block of material used to manufacture the cruciform specimen for the bending test. Young modulus and thermal expansion coefficient were also given as functions of temperature in the same criogenic temperature range.

A constant value of 0.3 was used for the poisson ratio over the whole temperature interval.

5.4 Implementation of the model in CAST3M

An elastic-plastic analysis aimed at simulating the post-test conditions of the CEA experiment was performed by ENEA using the PASAPAS procedure available in CAST3M.

The model was implemented through a dedicated subroutine conventionally named CRUNESC (CRUciform test for NESC-7 project), which is reported in Appendix 1.

The CRUNESC subroutine essentialy consists of three main sections.

The first section imports the geometry and the mesh previously created through a separate procedure named CRUGEN (CRUciform GENeration, not reported here).

The second section prepares all the input data for the PASAPAS procedure. In particular, it defines the type of mechanical model to use (elastic-plastic, isotropic) and the material properties needed by it. This section also applies the constraints and the loads to the specimen. Two types of loads are imposed: thermal load and mechanical load.

Thermal loads are applied by specifying a series of temperature snapshots with an imposed uniform field, each one corresponding to a loading step, so as to reproduce the temperature evolution along the LCF cycle (note that thermal equation is thus not solved). Since the temperature is uniform and the specimen is allowed to freely expand as a result of thermal dilatations, this type of load does not directly create any stress in the specimen. However, being all the material properties temperature dependent, it indirectly affects the results through non linear variation of the such properties.

Mechanical loads are applied by first creating their vector configuration (of unit module) and then multiplying it, at each loading step, by a proportional factor so as to reproduce the LCF loading path. Finally, once that all the input data are created, the PASAPAS procedure is

called to perform the elastic-plastic analysis. This is done in the third section of the CRUNESC procedure. A user-defined subroutine is also implemented within the PASAPAS routine to save the relevant data (CMOD, deflexion, temperature and load evolution) at each intermediate step.

An additional procedure was also developed to perform the post-processing data treatment after the PASAPAS calculation was completed. This subroutine calculates the J-integral (as a mean value along the 3-D crack tip) and the corresponding stress intensity factor Kj at every loading step. It also computes the local values of these quantities at every point of the crack tip for the last loading step (i.e., at fracture).

5.5 Simulation results

The simulation was performed on the ENEA High Performance Supercomputing Infrastructure CRESCO allowing the calculation to be completed in about 60 hours. The results obtained from the simulation are reported hereafter for the most significant parameters and compared to the experimental results coming from the CEA test.

The evolution of the mean Kj along the LCF cycle is shown in Fig. 5-9. It can be noted that during the cooling phase, when the load is kept constant, Kj decreases of about 2%. This due to the increase of the yield strength of the material with the decreasing of the temperature, which in turn results in the reduction of the plastic zone near the crack tip.

In Fig. 5-10, the calculated CMOD is shown as a function of the applied load and compared to the experimental values. A sufficient agreement is found, although some discrepancies arise in the final region of the preload phase and during cooling where the simulation tends to overestimate the CMOD, showing a higher compliance than the real one.
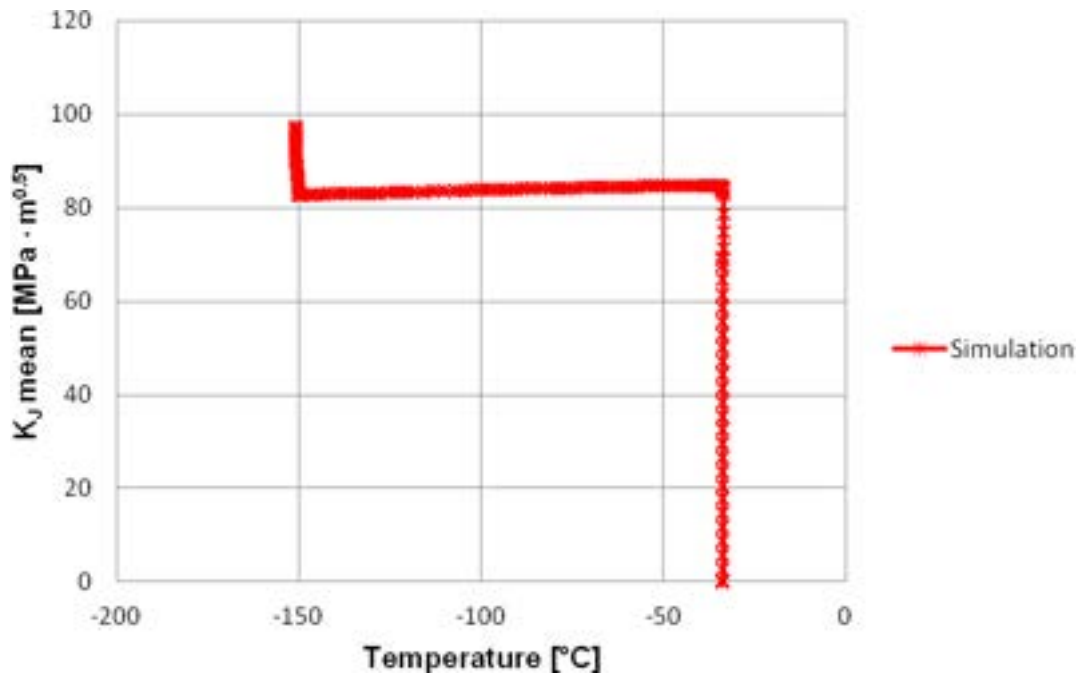
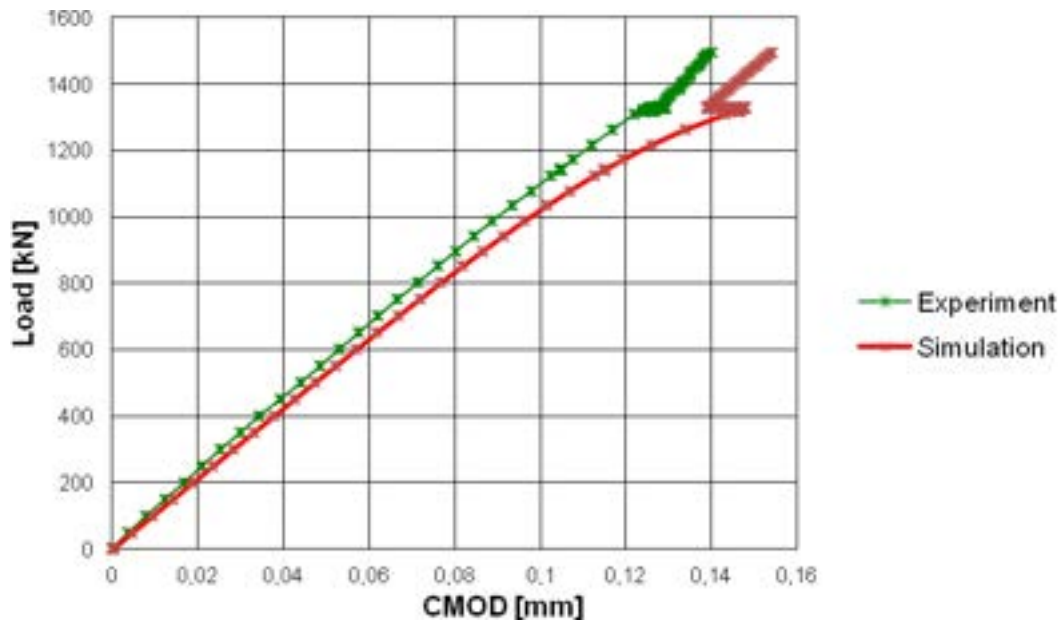Fig. 5-9 – Evolution of the calculated mean stress intensity factor

Fig. 5-10 – Load vs. CMOD

Finally, Fig. 5-11 shows the deflexion of the specimen as a function of the applied load, for both numerical simulation and experimental test. A very good agreement is obtained in this case all over the loading path.
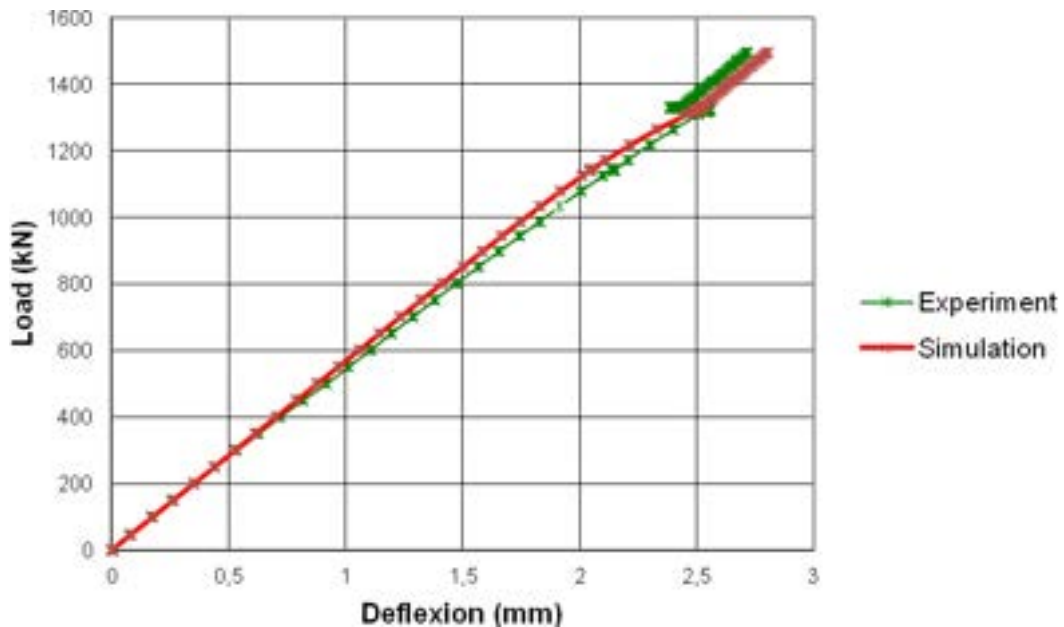

Fig. 5-11 – Load vs. specimen deflection

6. Conclusions

In the framework of the European NESC-7 project, a large scale test on a cruciform specimen of 18MND5 ferritic steel representative of a French PWR pressure vessel was performed at CEA-Saclay LISN laboratory to assess the beneficial effect of the WPS phenomenon under biaxial loading conditions typical of a PTS transient event. A LCF loading cycle was considered for the test. As a support to the test and within a close collaboration with CEA, a post-test analysis was conducted by ENEA through the simulation of the experiment by means of the CAST3M Finite Element code. Suitable procedures were developed to construct the geometry and the mesh and to carry out the calculation. An elastic-plastic fracture mechanics analysis was performed using the material properties provided by CEA within the NESC-7 community. The numerical results obtained are in general good agreement with the experimental ones, thus proving that the numerical tool developed is to be considered sufficiently reliable to simulate this kind of PTS tests.

References

[1] IAEA staff, *Pressurized Thermal Shock in Nuclear Power Plants: Good Practices for Assessment*, IAEA Technical Report, IAEA-TECDOC-1627, 2010

[2] IAEA staff, *Guidelines on Pressurized Thermal Shock Analysis for WWER Nuclear Power Plants*, IAEA Technical Report, IAEA-EBP-WWER-08 (Rev. 1), Vienna, 2006

[3] J.J. McGowan, *Application of Warm Prestressing Effects to Fracture Mechanics Analyses of Nuclear Reactor Vessels during Severe Thermal Shock*, Nuclear Engineering and Design, Vol. 51, pp. 431-444, 1979

[4] K. Wallin, *Master Curve Implementation of the Warm Pre-Stress Effect*, Engineering Fracture Mechanics, Vol. 70, No. 18, pp. 2587–2602, 2003

[5] R.D. Cheverton, ORNL/NUREG/TM-31 (September 1976)

[6] W.J. McAfee, B.R. Bass, J.W. Bryson Jr., W. E. Pennell, *Biaxial Loading Effects on Fracture Toughness of Reactor Pressure Vessel Steel*, USNRC Report, NUREG/CR-6273, 1995

[7] B B. R. Bass, J. W. Bxyson, T. J. Theiss, M. C. Rao, *Biaxial Loading and Shallow-Flaw Effects on Crack-Tip Constraint and Fracture Toughness*, USNRC Report, NUREG/CR-6132, 1994

[8] C. Jacquemoud, *NESC VII Project: 5 point bending tests on cruciform specimen – Experimental report on test 1 and 2*, CEA Technical Report, Référence DEN/DANS/DM2S/SEMT/LISN/RT/10-017/A, 2010

Annex 1 – CRUNESC procedure

```
******************************************************
**
**       CALCOLO PROVINO CRUCIFORME
**       (post-test analisi)
**       Percorso di carico LCF
**       Twps = -30 , Tfrac = -150, Kwps = 80
**
** ****************************************************


************************ PERSO1 ********************
DEBP perso1 TA2*TABLE ;

mess 'inizio PERSO1';

WTAB = TA2 . 'WTABLE';
tpas = WTAB . 'TEMPS0';
inpas= enti tpas;

Patt = extr load (inpas + 1);
Patt = Patt * 8 /1000;
Tatt = extr Tev  (inpas + 1);

mess 'Passo attuale = ' inpas;
mess 'Carico attuale = ' Patt;
mess 'T attuale = ' Tatt;


si (tpas NEG 0.);

depact  = TA2 . 'ESTIMATION' . 'DEPLACEMENTS' ;
pdeflex = vcroit2 POIN PROC (0. 325. 0.);

UYcl = extr depact UY pclip1 ;
UXdef = extr depact UX pdeflex;

opti rest 'out'; rest;

cmod = cmod et (prog (2*UYcl));
deflex = deflex et (prog UXdef);
passi = passi et (prog tpas);
Pstory = Pstory et (prog Patt);
Tstory = Tstory et (prog Tatt);
```

```
sinon;

cmod   = prog 0.;
deflex = prog 0.;
passi  = prog 0.;
Pstory = prog Patt;
Tstory = prog Tatt;

finsi;

OPTI SAUV 'out';
SAUV passi cmod deflex Pstory Tstory;

mess 'fine PERSO1';


FINP ;
**************************************************



**************************************************
* Recupero mesh
**************************************************
*
OPTI REST 'mesh12_x64.sauv' ;
rest;


**************************************************
* curve sigma-epsilon
**************************************************
opti acqu 'tensile.txt';

matb = table;
nc=6;
i=0;

* ciclo esterno sul numero di curve sigma-eps
repe cl0 nc;
i=i+1;
matb . i = table;

acqu n1*entier;
acqu t1*flottant;

* lettura degli n1 valori di epsilon
eps1 = prog;
```

```
repe cl1 n1;
acqu val1*flottant;
eps1 = eps1 et (prog val1);
fin cl1;

* lettura degli n1 valori di sigma
sig1 = prog;
repe cl2 n1;
acqu val2*flottant;
sig1 = sig1 et (prog val2);
fin cl2;

ev1 = evol manu 'eps' eps1 'sig' sig1;

* calcola modulo di Young
eps1_y = extr (extr ev1 ABSC) 2;
sig1_y = extr (extr ev1 ORDO) 2;
myoung = (sig1_y/eps1_y);

*dess ev1;
matb . i . 'temp' = t1;
matb . i . 'evol' = ev1;
matb . i . 'E' = myoung;

fin cl0;

tens1 = matb . 1 . 'evol';
tens2 = matb . 2 . 'evol';
tens3 = matb . 3 . 'evol';
tens4 = matb . 4 . 'evol';
tens5 = matb . 5 . 'evol';
tens6 = matb . 6 . 'evol';

T1 = matb . 1 . 'temp';
T2 = matb . 2 . 'temp';
T3 = matb . 3 . 'temp';
T4 = matb . 4 . 'temp';
T5 = matb . 5 . 'temp';
T6 = matb . 6 . 'temp';

traz1 = nuag comp T T6 T5 T4 T3 T2 T1 comp trac tens6 tens5 tens4
tens3 tens2 tens1;


*************************************************
* CALCOLO ELASTO-PLASTICO
*************************************************
```

```
* Coeff. Poisson *
nu1 = 0.3;

* modulo di Young
E1 = matb . 1 . 'E';
E2 = matb . 2 . 'E';
E3 = matb . 3 . 'E';
E4 = matb . 4 . 'E';
E5 = matb . 5 . 'E';
E6 = matb . 6 . 'E';
ptemp  = prog T6 T5 T4 T3 T2 T1;
pyoung = prog E6 E5 E4 E3 E2 E1;

evy = evol manu 'T' ptemp 'YOUN' pyoung;
*dess evy;

* Coeff. dilatazione termica *
ptemp  = prog -196. -150. -125. -100. -75. -50. -25. 0. 20. 100.;
palpha = prog  9.45e-6 9.80e-6 9.98e-6 10.16e-6 10.34e-6
          10.51e-6 10.69e-6 10.87e-6 11.037e-6 11.6e-6 ;

eva = evol manu 'T' ptemp 'ALPH' palpha ;


*-----------------------------------
** Modello meccanico e materiale **
*-----------------------------------
mocroi2  = MODE vcroit2 MECANIQUE ELASTIQUE PLASTIQUE ISOTROPE;
matcroi2 = MATE mocroi2 'YOUN' evy 'NU' nu1 'ALPH' eva 'TRAC' traz1;


*-----------------------------------
** Condizioni ai limiti **
*-----------------------------------
cl1 = BLOQ UX scharg1;
cl2 = BLOQ UY ssxoz;
cl3 = BLOQ UZ ssxoy;
clcroi2 = cl1 ET cl2 ET cl3 ;


*-----------------------------------
** evoluzione carico meccanico **
*-----------------------------------

preload = prog 0. 2.2111 2.2922 48.6074 98.8972 149.1059 199.3956
249.6043 299.8940 350.0215 400.2302 450.5200 500.6475 551.0184
601.3082 651.5979 701.8066 752.0963 802.3050 852.5137 897.3689
942.9542 988.5394 1033.7191 1079.3855 1124.8086 1143.3833 1143.2211
```

```
1142.0856 1141.3555 1140.9500 1172.3406 1217.8447 1263.1866
1308.8530 1324.8323 1322.0745 1320.6956 1319.8843 1318.9922
1318.5055 1318.0999 1317.5321 1328.8879;

cooling1 = prog 1328.8068 1328.8879 1328.8879 1328.7257 1328.7257
1328.8879 1328.9690 1328.8879 1328.8068 1328.8068 1328.7257
1328.8068 1328.8068 1328.9690 1328.8068 1328.8068 1328.7257
1328.8879 1328.8068 1328.8068 1328.8068 1328.6445 1328.8879
1328.8879 1328.7257 1328.8068 1328.8068 1328.8068 1328.8880
1328.8879 1328.8879 1328.8879 1328.9690 1328.8879 1328.8879
1328.8879 1328.8879 1328.8879 1328.8879 1328.8879 1328.7257;

cooling2 = prog 1328.8879 1328.7257 1328.8879 1328.8879 1328.8068
1328.7257 1328.9690 1328.8879 1328.8879 1328.8879 1329.0502
1328.8068 1328.8879 1328.8068 1328.8068 1328.8068 1328.9690
1328.8879 1328.8879 1328.8068 1328.8068;

cooling = cooling1 et cooling2;

fracture = prog 1331.6458 1338.3781 1345.1915 1351.6805 1358.4128
1365.1453 1371.6343 1378.3666 1384.9368 1391.8313 1398.5636
1405.1338 1411.7039 1418.4363 1425.0875 1431.5765 1438.4711
1444.9601 1451.6113 1458.3436 1464.9138 1471.6461 1478.2163
1484.8676 1491.4376 1496.7911;

* creazione percorso di carico
npre = dime preload;
ncool = dime cooling;
nfract = dime fracture;

stpre = prog 0 pas 1 (npre - 1);
stcool = prog npre pas 1 ((npre - 1) + ncool);
stfract = prog (npre + ncool) pas 1 (npre + ncool + nfract - 1);

stload = stpre et stcool et stfract;
load = preload et cooling et fracture;

* x 1000 per avere kN -> N e poi divido per 8 per la simmetria
load = (load*1000.)/8;

evload = evol manu stload load;

* versore del carico sui 2 bracci
fcroi1 = FORC FX (1.) lch1;
fcroi2 = FORC FX (1.) lch2;

charm1 = CHAR 'MECA' fcroi1 evload;
charm2 = CHAR 'MECA' fcroi2 evload;
```

31

```
*-----------------------------------
** evoluzione carico termico **
*-----------------------------------


Tev1 = prog -33.61 -33.61 -33.63 -33.62 -33.65 -33.66 -33.69 -33.72
-33.68 -33.69 -33.70 -33.72 -33.72 -33.73 -33.72 -33.70 -33.70 -33.71
-33.66 -33.65 -33.66 -33.67 -33.63 -33.65 -33.66 -33.65 -33.66 -33.63
-33.61 -33.60 -33.59 -33.57 -33.57 -33.57 -33.57 -33.60 -33.54 -33.66
-33.95 -33.79 -33.78 -33.92 -33.87 -33.97 -34.54 -35.10 -35.86 -37.13
-38.19 -39.50 -40.73 -42.24 -43.84 -45.29 -46.80 -48.30 -50.02 -51.79
-53.55 -55.37 -57.16 -59.14 -61.17 -63.10 -65.34 -67.55 -69.61 -71.93;

Tev2 = prog -74.31 -76.67 -78.83 -80.98 -83.60 -86.06 -88.62 -90.90
-93.15 -95.38 -97.63 -99.96 -102.30 -104.56 -107.04 -110.32 -113.11
-115.84 -118.76 -120.96 -123.24 -125.35 -128.01 -129.17 -130.80
-132.80 -134.72 -137.08 -139.29 -141.58 -143.53 -145.53 -147.19
-149.24 -149.92 -149.93 -149.98 -150.03 -150.14 -150.18 -150.28;

Tev3 = prog -150.29 -150.29 -150.32 -150.38 -150.51 -150.57 -150.60
-150.71 -150.84 -150.85 -150.90 -150.89 -150.89 -150.92 -150.88
-150.85 -150.88 -150.86 -150.84 -150.79 -150.81 -150.85 -150.98;

Tev = Tev1 et Tev2 et Tev3;

tabtps = TABLE ;
tabT = TABLE ;

lun = dime stload;

repe cl3 lun;
jj = &cl3;
tabtps . (jj - 1) = extr stload jj;
tabT   . (jj - 1) = MANU 'CHPO' vcroit2  1 'T' (extr Tev jj);
fin cl3;

chart2 = CHAR 'T' tabtps tabT ;


** Calcolo PASAPAS **
*-----------------------------------
TAB1 = TABLE ;
TAB1.'MODELE' = mocroi2 ;
TAB1.'CARACTERISTIQUES' = matcroi2 ;
TAB1.'BLOCAGES_MECANIQUES' = clcroi2 ;
TAB1.'CHARGEMENT' = (charm1 ET charm2 ET chart2);
TAB1.'CONVERGENCE_FORCEE' = faux ;
TAB1.'TEMPERATURES.0' = MANU 'CHPO' vcroit2  1 'T' (-33.61);
TAB1.'TALPHA_REFERENCE' = -33.61 ;
```

```
**
TAB1.'GRANDES_DEFORMATIONS' = faux ;
TAB1.'GRANDS_DEPLACEMENTS' = faux ;
**
TAB1.'MES_SAUVEGARDES' = table ;
TAB1.'MES_SAUVEGARDES'.'DEFIN' = vrai ;
TAB1.'MES_SAUVEGARDES'.'DEFTO' = vrai ;
TAB1.'PROCEDURE_PERSO1' = vrai ;

TAB1.'TEMPS_CALCULES' = stload  ;

PASAPAS TAB1;

opti sauv 'lcf1.tab';
sauv TAB1;


FIN;
```